agronomy

MDPI

Article

Experiment and Study of Garlic Root Cutting Based on Continuous Force Feedback

Ke Yang [1], Zhaoyang Yu [1,2], Weiwen Luo [1], Jiali Fan [1], Yuyao Li [1], Fengwei Gu [1], Yanhua Zhang [1], Shenying Wang [3], Baoliang Peng [2,*] and Zhichao Hu [1,*]

[1] Nanjing Institute of Agricultural Mechanization, Ministry of Agriculture and Rural Affairs, Nanjing 210014, China
[2] Key Laboratory of Modern Agricultural Equipment, Ministry of Agriculture and Rural Affairs, Nanjing 210014, China
[3] College of Biosystems Engineering and Food Science, Zhejiang University, Hangzhou 310058, China
* Correspondence: pengbaoliang@caas.cn (B.P.); huzhichao@caas.cn (Z.H.)

Abstract: In this study, we quantified and analyzed the root-cutting process of garlic with a test bench with pressure sensors on the basis of the comparative analysis of various information perception methods. On the basis of the output value of the pressure sensor, the force curve of garlic roots was plotted, and the double round blade cutting module is optimized on the basis of the force curve diagram. The innovative proposal of slotted round blades for garlic root cutting is presented here. The round blade diameter is 110 mm, the center distance is 100 mm, the blade thickness is 1 mm, and the blade speed is 1200 r/min. According to the analysis of the force curve, it was found that the slotted round blade with the slanted blade could generate a strong thrust to cut the roots. The cutting effect was better and the cutting surface of the roots was straight. The slotted blade meets the need for cutting garlic roots.

Keywords: pressure sensors; pressure graphs; round blade; cutting root; garlic; test bench

Citation: Yang, K.; Yu, Z.; Luo, W.; Fan, J.; Li, Y.; Gu, F.; Zhang, Y.; Wang, S.; Peng, B.; Hu, Z. Experiment and Study of Garlic Root Cutting Based on Continuous Force Feedback. *Agronomy* **2023**, *13*, 835. https://doi.org/10.3390/agronomy13030835

Academic Editors: Anastasios Darras and Paul Kwan

Received: 1 February 2023
Revised: 23 February 2023
Accepted: 10 March 2023
Published: 13 March 2023

1. Introduction

Garlic (*Allium sativum* L.) is a widely grown vegetable condiment with both edible and medicinal values [1–4]. Studies have shown that garlic consumption is effective in reducing the risk of diseases such as hypertension and diabetes [5,6]. In addition to its disease-prevention function, garlic has antibacterial, anti-inflammatory, and insecticidal properties [7–10]. The organosulfur compounds and polyphenols contained in garlic give it a unique flavor [11]. It is the unique flavor and the well-known medicinal value of garlic that have made it the most important seasoning vegetable in the world [12].

Currently, root cutting during garlic harvesting must be carried out manually, resulting in low-efficiency of garlic harvesting, and there is an urgent need to break through the bottleneck of mechanized and automated root-cutting technology [13–16]. However, the size of bulbs and the density of garlic roots vary due to the different sizes and biological activities of garlic seeds used for cultivation and the different water, fertilizer, and light conditions during the growth of garlic. Garlic roots are the cutting objects of root cutting. It is necessary to quantify the difference in cutting effect due to the variability of cutting objects in this study. The analysis of the cutting effect is the key to evaluating the different cutting methods. Whether a scientific and reasonable quantitative analysis method can be found will directly affect the research on garlic-cutting tools.

Computer analyses are usually used to analyze complex problems in agricultural equipment research [17–22]. However, for the study of garlic root cutting, computer simulation analysis cannot simulate the stochastic nature of garlic root characteristics. Therefore, the root-cutting process must be studied by employing quantitative analysis of information perception during the actual experiment. The experimental study of vibration damping of

thresher support beams in combined harvesters using acceleration sensors and accompanying signal acquisition and processing systems was conducted to explore the vibration damping effect of different structures [23]. Pressure sensors were used as a means to obtain the biomechanical properties of sorghum stems and an innovative approach to studying the biomechanical properties of anisotropic materials through the testing of engineering materials [24]. The developed cotton stalk discrete element model using pressure sensor experimental testing and discrete element modeling can serve as a basis for the simulation of related operating machinery, including uprooting and processing machinery [25]. The installation of piezoelectric sensors on harvesters can effectively identify grain shocks from vibration noise [26]. Real-time detection of clamping force by pressure sensors on the end-effector enables picking and non-destructive collection of kiwis [27]. The mechanical properties of potato tubers grown in different soils were quantified with the help of a test machine with pressure sensors on the test head [28]. An innovative method was developed to reliably measure the transverse Young's modulus of the pith and outer bark tissue of maize stems, and the validity of the method was finally verified by pressure transducer testing [29]. Using a test setup with a pressure sensor, it was demonstrated that different pressure values applied during the extraction of pomegranate juice can yield different quality products [30]. More details of the biomechanical properties of sweet sorghum were revealed with the help of pressure sensors [31]. The values and variation patterns of biomechanical properties of Laver (*Porphyra yezoensis* Ueda) were obtained by a combination of morphological and mechanical tests and numerical statistics [32]. The shear, compression, and bending characteristics of sorghum (*S. bicolor*) straw in the straw and seed stages were determined using a universal testing machine with a pressure transducer as the core component [33]. A pressure sensor was used to study the mechanical properties of the compression response of bamboo fibers, the compression process was visualized and quantified, and the robustness of the method was verified by the constructed intrinsic structure model [34]. The Young's modulus of wood chip particles was studied using a test apparatus with a pressure transducer as the core working part, and the deformation curves of wood chip particles under different compressive stresses were plotted [35]. A test apparatus using a pressure sensor as a core working component demonstrated that foliar fertilizer application increased the strength of the seeds and their ability to resist mechanical damage under quasi-static loading [36]. Comparison of the different cutting tools showed that the high-speed rotating circular blade disc was able to cut the weeds effectively [37]. It is clear that the measurement results of pressure sensors are authoritative, and the study of the mechanical properties of objects utilizing pressure sensors is a time-tested method.

Force sensors were used to accurately measure the force of grasping apples and to perceive information about apples with irregular shapes and fragile properties [38]. Using deep learning to perceive information about the shape of garlic and automatically adjusting the digging depth of the garlic combine harvester can reduce the workload of operators [39]. Quantitative analysis of kiwi fruit hardness is achieved by smart haptic sensors [40]. Whether the object is an agricultural product or a domestic animal, or even a person, information about the object can be sensed scientifically using appropriate sensors. However, in direct contact scenarios, information about the forces applied often accurately describes the changes in the object's characteristics. The use of force sensors and inertial measurement units to sense the picking force and motion required to pick mushrooms allows for quantitative analysis of the picking process [41]. To enhance the detection of objects by robotic hands, force sensors are popularly used to obtain information about objects [42–44]. The output value of a force sensor changes over time, and the change in output value often marks a change in the state of the object. Therefore, force sensors can detect changes in the state of an object in real-time.

This study was conducted to investigate the mechanism of interaction between the double round blades and garlic roots when cutting garlic roots to improve the operational efficiency of garlic combine harvesters. Since garlic roots are bundles of root whiskers, and each garlic root bundle is different from the others, this study poses a great challenge.

Considering various research tools, a force sensor was used to sense the external force on the garlic roots during the root-cutting process. The process of force change on the garlic root was quantified by the variation of the force sensor measurements on the time axis. The root-cutting mechanism based on double round blades was investigated by analyzing the whole root-cutting process. On the basis of this, the double round blades were optimized to double-slotted round blades to improve the cutting effect of garlic roots. The structural parameters and operating parameters of the double-slotted round blade were obtained.

2. Materials and Methods

Usually, the garlic root we see is just the whiskers of the garlic. As shown in Figure 1, when a clove of mature garlic is cut open along the axis of the stalk, it is found that the cloves grow on the root disc and the root whiskers grow down from the root disc. The garlic root includes the root disk and the root whiskers. Generally, skilled workers use special scissors to cut the root disk and complete the cutting of the root. Cutting the root disc is the most efficient way to cut the roots and can remove a large number of root whiskers at one time. However, the study of mechanical root-cutting needs to deal with many possibilities, and the designed root-cutting device must be able to overcome the problems that exist in many possibilities. Root discs are hard, while root whiskers are long and soft. The cutter module needs to be suitable for removing both the root disc and the root whiskers. All garlic plants were sourced from the garlic planting base in Jinxiang County, Nanjing Institute of Agricultural Mechanization, Ministry of Agriculture and Rural Affairs. Jinxiang has a long history of garlic cultivation and encompasses a large area. To retain the moisture of the garlic roots, the roots were completely wrapped with soil after the garlic was excavated out of the soil at the planting base.

Figure 1. Garlic plant in a field. The garlic cloves form the bulb of garlic. The garlic root includes the rooting site and the root whiskers.

Field excavations were conducted on garlic from a field located at 34°59′59″ N, 116°14′55″ E. The treated test samples were delivered to the laboratory within 3 days for root-cutting tests. A total of 200 strain samples were sent to the laboratory. From these 200 samples, a random selection method was used to determine the test subjects for the root-cutting test [45]. The moisture content of the garlic roots used for the root cutting test was measured to be 85.20–90.12%. On the basis of existing studies, it is known that the Poisson's ratio of the bulb is 0.23, and the elastic modulus is 2.382×10^7; the Poisson's ratio of the root is 0.385, and the elastic modulus is 2.26×10^6 [13].

2.1. Garlic Root-Cutting Test Bench

The garlic root-cutting test bench consists mainly of a clamping and conveying mechanism, motion control system, root-cutting knife system, pressure measurement and recording system, and test bench frame, as shown in Figure 2. The clamping and conveying mechanism use a linear slide module (FBL60E900135, FUYU, Chengdu, China) for conveying garlic seedlings, and the driving force for conveying is provided by a stepper motor (57CM18, Rtelligent, Shenzhen, China). The motion-controlled system senses the clamping and conveying position by proximity switch (TL-Q5MC1, OMCH, Wenzhou, China), the STM32F103 microcontroller realizes the motion control, and the human–machine interaction is realized by using the controller handle whose housing is printed by 3D. The root cutter system consists of a cutter module and a root cutter governor, and the root cutter governor can adjust the speed of the double-round blades. The pressure measurement and recording system consist of a pressure sensor (DYZ101, DAYANG SENSOR, Bengbu, China), a pressure transmitter (DY220, DAYANG SENSOR, Shenzhen, China), and a computer; it can complete pressure measurement to signal to process, and finally, finish the work of displaying and keeping data. The test stand frame is built from aluminum alloy profiles, the parts are processed after 3D modeling by computer in the early stage, and the parts are assembled after the processing is completed, which is called the test stand frame.

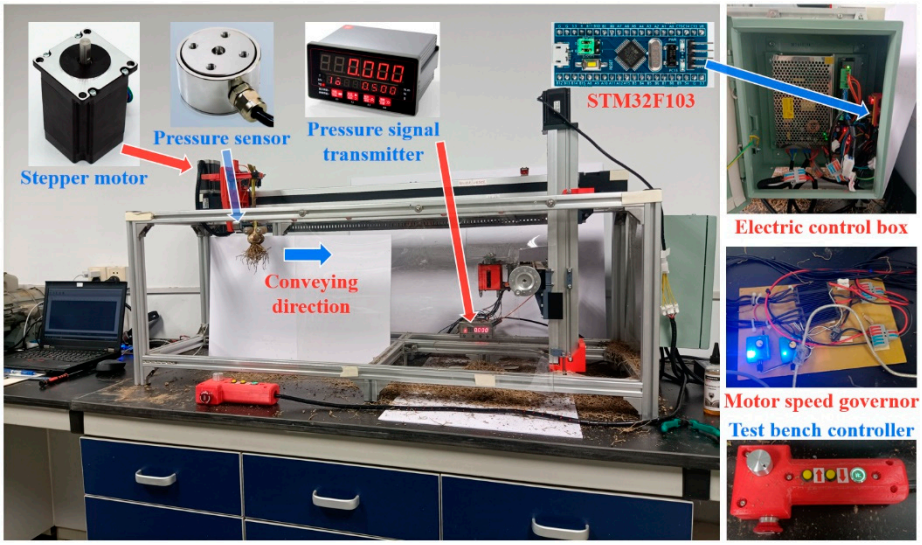

Figure 2. Schematic diagram of the test bench structure.

2.2. Cutter Module

The cutter module consists mainly of brushless direct current motor (BLDCM) (LA3620 KV50, Eaglepower, Zhongshan, China), lower fixing plate, upper fixing plate, motor mount, connecting shaft, bearing (6905RS, ZY Bearings, Shanghai, China), round blade, fastening shims, rear fixing plate, and cooling fan (AD0524HB-G70, ADDA CORP RATION, Beijing, China), as shown in Figure 3.

The lower fixing plate and upper fixing plate are made of carbon-fiber-reinforced organic composite material processed by a computer numerical control machine, which has the characteristics of high strength and lightweight. The motor mount and rear fixing plate are 3D-printed and made of polymer material with lightweight and high functional integration. The connecting shaft is made of aluminum alloy, which is lighter than steel and has better thermal conductivity and higher strength than plastic. After preliminary experiments, we decided to use a round blade with a disc and a round blade with two cutting angles as the research objects. The round inserts were custom-machined from 9CrSi alloy. The equipped cooling fan is used to dissipate heat for the BLDCM to avoid high-temperature damage and blow away the dust and residue attached to the BLDCM.

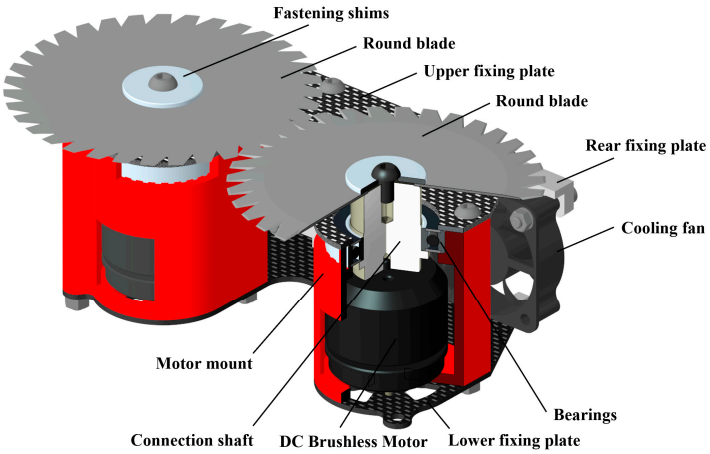

Figure 3. Schematic diagram of the structure of the cutter module.

The BLDCM used in the study is an external rotor motor. The bottom of the BLDCM is bolted to the bottom plate of the motor mount. The connecting shaft is bolted to the top of the outer rotor of the BLDCM. The top of the motor mount is provided with bearing mounting holes. The shaft is rotated relative to the motor mount by the bearing. The bolts that press the upper fixing plate and the lower fixing plate pass through the bolt holes on the motor mount to fix the upper fixing plate, the lower fixing plate, the bearing, the motor mount, the connecting shaft, and the BLDCM together. At the same time, the bolts that press the upper fixing plate and lower fixing plate pass through the threaded holes on the rear fixing plate to fix the upper fixing plate, lower fixing plate, and rear fixing plate together. The heat dissipation fan is fixed to the rear fixing plate by bolts. The bolt through the fastening shims fixes the round blade to the top surface of the connecting shaft.

When the cutter module operates, the motor drive plate drives the BLDCM to rotate, and the connecting shaft driven by the BLDCM drives the round blade to rotate. The connecting shaft with bearings can run smoothly. The BLDCM is not subjected to radial force and overturning torque, and the radial force on the round blade is carried by the bearing.

2.3. Determination of Main Parameters

For purpose of comparing the cutting capacity, a double round blade was first selected for the study. The parameters of the double round blade root-cutting mechanism are divided into structural parameters and working parameters. The structural parameters include mainly the diameter of the round blade D, thickness h, edge angles φ_1 and φ_2, pre-processing thickness h_0, etc., as shown in Figure 4. The working parameters are mainly the blade speed n, the overlap area width (the maximum overlap width of two blades) B, the overlap area length (the maximum overlap length of two blades) l, the center distance of the blade l_0, etc.

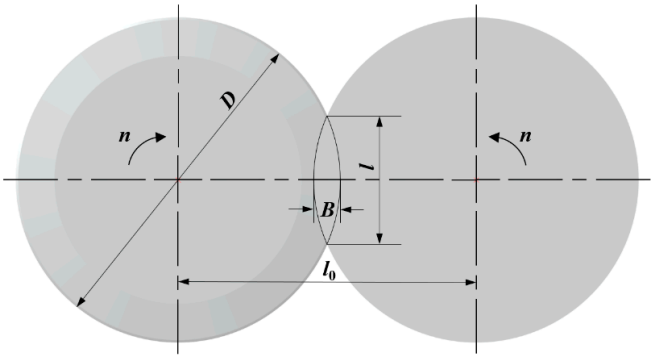

Figure 4. Parameters of the double round blade.

The structural parameters and working parameters of the round blades directly determine the root-cutting effect of the cutter module, which should be as compact, low-energy-consuming, and reliable as possible while meeting the requirements of root-cutting capacity [37].

In the previous experiment, the maximum value of bulb diameter d_{max} measured on 200 garlic seedlings was 63.86 mm, the standard deviation of bulb diameter was 5.45, and the coefficient of variation was 0.11. The diameter of the fastening spacer d_p was 28 mm for the bulb to pass smoothly between the two fastening spacers when cutting the roots, and the center distance l_0 of the round blade should satisfy

$$l_0 > d_{max} + d_p \tag{1}$$

The round blade center distance l_0 should be greater than 91.86 mm, considering the error of aligning the root cutter module with the target when cutting the root, and the round blade center distance l_0 should be enlarged appropriately. In addition, to make the root cutter module compact, the round blade center distance l_0 should not be too large. The center distance of double round blades l_0 = 100 mm is chosen.

After determining the round blade center distance l_0, further consideration of other structural parameters is required. Due to the bi-directional shear force, a better cutting effect can be achieved by using overlapping round blades. The overlapping area width B determines the size of the overlapping area length l. A smaller overlap area width B will result in insufficient overlap area length l, which will hurt the cutting result. A larger overlap area width B will reduce the cutting effect of the blade's normal thrust at the beginning of the cut, which will also hurt the cutting effect. Therefore, after a preliminary test, the overlap area width B is determined to be 10 mm, and the round blade diameter D is 110 mm. Then, the overlap area length l is calculated as follows:

$$l = 2 \times \sqrt{(D/2)^2 - (D/2 - B/2)^2} \tag{2}$$

Substituting the data, the length of the overlapping area l = 45.8 mm can be calculated.

2.4. Analysis of the Effective Cutting Speed of Round Blades

Since the double-round blades rotate in the same plane, a single-round blade can be taken as the object of study when analyzing the motion trajectory of the cutting point on the round blade. The origin O of the coordinate system is set at the center of rotation of the round blade, the x-axis direction is the same as the clamping and conveying direction, and the y-axis direction is shown in Figure 5. The speed of clamping and conveying is v_m, and the direction is shown in Figure 5. Suppose the cutting point is at A at a certain moment; after time t1, the cutting point changes from A to B, and θ is the angle of change of the cutting point. After time t2, the cutting point changes to C, and γ is the angle of change of the cutting point, at which time the linear velocity v_c of the cutting point C is in the same direction as v_m. After time t3, the cutting point changes to D, δ is the angle of change of the cutting point, and the linear velocity of each cutting point is shown in Figure 5.

Since the components of the cutting line velocity of the double round blade acting on the garlic root in the y-direction cancel each other, only the components of the line velocity of each cutting point in the x-axis direction are analyzed. Then, we have the following:

$$v_{Ax} = v_A \cdot \sin\beta \tag{3}$$

$$v_{Bx}(t) = v_B \cdot \sin(\beta + \omega t) \tag{4}$$

$$v_{Cx} = v_C \tag{5}$$

$$v_{Dx}(t) = v_D \cdot \cos(\beta + \omega t - \pi/2) \tag{6}$$

$$v_A = v_B = v_C = v_D = \pi n D/60 \tag{7}$$

$$\sigma = v_x / v_m \tag{8}$$

where v_{Ax}, v_{Bx}, v_{Cx}, and v_{Dx} are the components of the cutting line velocities v_A, v_B, v_C, v_D in the x-axis direction at the cutting points A, B, C, and D, respectively; β is the angle between the line connecting the cutting point A and the origin O of the coordinate system and the x-axis, rad; ω is the angular velocity of rotation of the round blade, rad/s; n is the rotational speed of the round blade, r/min; D is the diameter of the round blade, m; σ is the speed ratio coefficient; v_m is the clamping transport speed, m/s; and v_x represents the component of the cutting point speed in the x-axis direction.

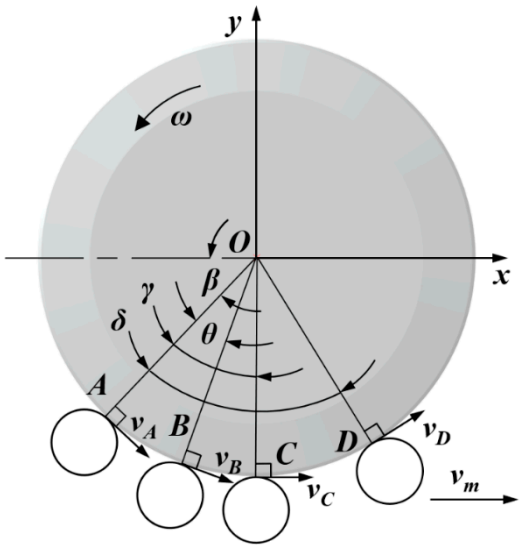

Figure 5. Analysis of the effective cutting speed of round blades.

According to Equations (3)–(5), it can be seen that during the change of the cutting point from A to C, the component of the line velocity of the cutting point in the x-axis direction gradually becomes larger, and the velocity component at the cutting point C achieves the maximum value v_C; after the point, C, the component of the line velocity of the cutting point in the x-axis direction gradually decreases. The component of the line velocity of the cutting point in the x-axis direction is called the effective cutting velocity v_x. Then, the effective cutting velocity v_x shows a change process of increasing and then decreasing during the change from cutting point A to cutting point D.

The speed ratio coefficient σ indicates the matching relationship between the effective cutting speed and the clamping and conveying speed, and the v_x/v_m value is the key to evaluating the cutting quality. By investigating the indicators of garlic combined harvesting operation, the maximum value of clamping and conveying speed was determined to be 0.75 m/s [16]. Thus, it can be seen that the rotational speed of the round blade is an important parameter affecting the cutting quality. A rotation speed of the round blade that is too low will lead to a low relative speed between the round blade and the garlic root, and the root will not be cut and congested; a rotation speed that is too high will reduce safety and increase energy consumption.

2.5. Round Blade Speed and Thickness

Considering the working round blade as a flywheel with a certain amount of energy stored, the energy it has when it rotates is

$$E = I\omega^2 K \tag{9}$$

$$I = \frac{GD^2}{4g} \tag{10}$$

$$G = \frac{\pi}{4} D^2 h \rho \tag{11}$$

$$\omega = 2\pi n \tag{12}$$

E is the energy of the round blade, J; I is the rotational inertia of the round blade, kg·m^2; K is the speed fluctuation coefficient, taken as 0.64; G is the mass of the round blade, kg; and ρ is the density of the round blade (material is 9CrSi), kg/m^3.

The joint vertical can be derived from the thickness of the round blade as

$$h = \frac{4gE}{\pi^3 D^4 n^2 \rho K} \tag{13}$$

Since there are few studies on garlic root cutting, the reference energy required to cut off a unit area of carrot stem and leaves was 3.1 J [46]. The energy required to cut carrot stems and leaves was calculated as the energy required to cut garlic roots.

Then, the energy that the round blade has when the garlic root is cut is

$$E = A \cdot E_k \tag{14}$$

$$A = \frac{1}{12} \pi D^2 \tag{15}$$

where E_k is the energy required to cut off the unit area of garlic root, J; and A is the average area of garlic root, cm^2.

Too thick a round blade will lead to larger inertia and affect the safety of cutting the roots. According to the relationship between the blade speed n and the cutting line speed of the blade, the cutting line speed of the blade is 6.908 m/s. The thickness of the blade is 1 mm, and the blade speed is 1200 r/min.

Due to the high rotational speed of the round blade at work, a direct collision of the blades of a rotating round blade at high speed would be destructive. It is foreseeable that a direct collision between a pair of rotating blades will cause damage to the cutting edge and even cause the blades to fly out quickly. A rapidly flying blade will cause unimaginable damage to people and machine parts around it. Therefore, measures must be taken to prevent collisions between rotating blades.

From Figure 6, it can be seen that opening the edge of the round insert on one side can effectively avoid the collision of the knife edge. When processing the round insert, the blank is a round steel piece with a diameter of 110 mm and a thickness of 1 mm. First, the edge angle $\varphi_1 = 3.5^\circ$ is polished, and the thickness of pre-treatment $h_0 = 0.2$ mm; then, the edge angle $\varphi_2 = 17^\circ$ is polished in the post-treatment.

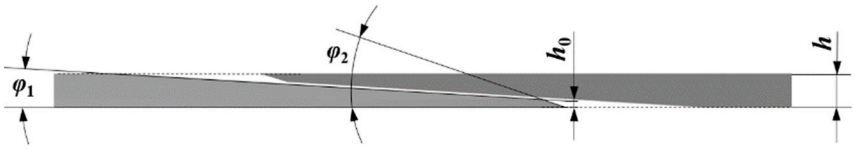

Figure 6. Parameters of the overlapping area of the double round blades.

With this processing method, the structural strength of the blade is ensured, and a sharp edge is obtained. At the same time, it can allow staggered installation of the upper and lower blades in the same plane due to the existence of blade bevel, which avoids the blade edge-to-edge collision, improves the safety, and always maintains the gap between the upper and lower blade edge at 1 mm. So far, the structural parameters of the double round blade root-cutting mechanism have been determined.

2.6. Analysis of Root-Cutting Force

The double round blade root-cutting machine is the core working part of the garlic root-cutting device. It determines the root-cutting effect and garlic clove damage of the

garlic root-cutting device, and the root-cutting resistance and cutting speed should be considered for the smooth cutting of garlic root to be achieved.

The double-blade root-cutting mechanism consists of two blades that overlap each other (acting directly on the garlic root) and each rotates at the same speed in reverse. When the garlic plant is fed from the clamping and conveying mechanism into the double round blade root-cutting mechanism, the loose root beads are squeezed and tightly bound together to form root bundles. Since the study ensured that the stalk was perpendicular to the clamping and conveying direction, the root whisker bundle before root cutting was assumed to be perpendicular to the clamping and conveying direction. For analysis, it is assumed that the cross-section of the cut part of the root bundle is a positive circle or an ellipse. When the root bundle is normal to the plane in which the blade is located at the moment when the cutting is completed, the cutting cross-section is a positive circle; when the root bundle is normal to the plane in which the blade is located, the cutting cross-section is an ellipse.

When being cut, the root bundle is subjected to the normal thrust force N and tangential slip force F. Assuming that the normal thrust force N_1 and N_2 and the tangential slip force F_1 and F_2 are applied to the root bundle by the two blades, the root bundle is also subjected to the tension force F_t along the clamping delivery direction, and the force analysis is shown in Figure 7.

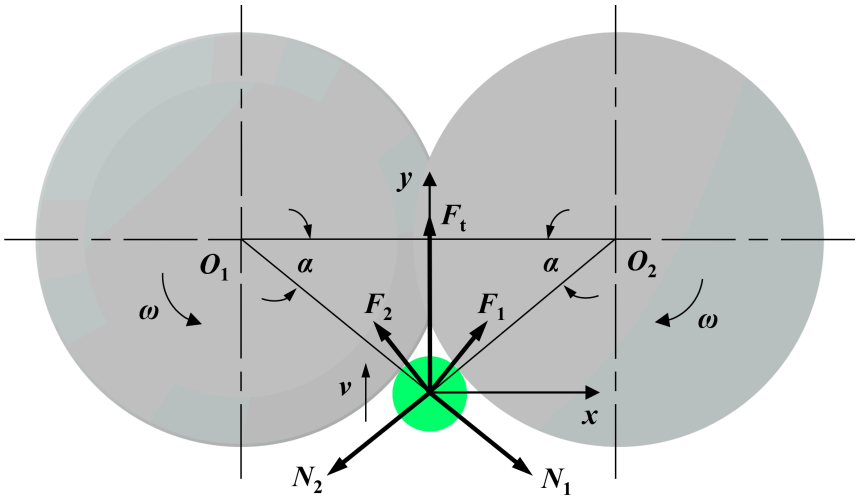

Figure 7. Schematic diagram of the force analysis of the garlic root.

The root bundle moves in the direction of velocity v. For the garlic root bundle to enter the double round blade root-cutting mechanism and be cut off without slipping when it touches the blade, the combined force on the y-axis should be satisfied in the same direction as the velocity v, i.e., the following conditions should be satisfied:

$$F_t > N_1 \sin\alpha + N_2 \sin\alpha - F_1 \cos\alpha - F_2 \cos\alpha \tag{16}$$

$$\alpha = \cos^{-1}\left[a/(D+d)\right] \tag{17}$$

where α is the angle between the normal thrust of the round blade and the line connecting the center of the round blade, (°); a is the distance between the centers of the two round blades, mm; D is the diameter of the round blade, mm; and d is the diameter of the cutting part of the garlic root beard bundle, mm.

Considering the different mechanical properties of root discs and root whiskers, they need to be analyzed separately. During the clamping and conveying process, the root disc does not oscillate significantly after the force is applied to the root disc because the root disc is a hard tissue after lignification. In the case that Equation (16) is satisfied, the root disc can be cut off smoothly by the double round blade root-cutting mechanism. However,

the root bundle composed of root whiskers is soft and will oscillate with the force, and the amplitude of oscillation is positively correlated with the magnitude of the force within a certain range. Therefore, the combined forces on the root bundle during the cutting process are the normal thrust N_1 and N_2 of the root bundle, the tangential slip forces F_1 and $F_{2,}$, and the internal tissue linkage force, which satisfy the following relationship in the positive y-axis direction:

$$F_k = F_1\cos\alpha + F_2\cos\alpha - N_1\sin\alpha - N_2\sin\alpha - F_n \quad (18)$$

where F_k is the component force of the combined force on the root whisker bundle in the positive y-axis direction, and F_n is the component force of the internal tissue linkage force in the positive y-axis direction.

The internal tissue linkage force F_n varies depending on the root bundle and is difficult to quantify and analyze. Therefore, a tensile force sensor was applied in the study to quantify and visualize the whole root-cutting process.

3. Results

3.1. Double Round Blade Root-Cutting Test

The fingers installed on the test bench were of the same structure as those installed on existing garlic combine harvesters [47,48]. After the garlic plant was fixed on the clamping conveyor, the garlic stems were placed between the two fingers and the bulbs were placed against the two fingers, as shown in Figure 8. To be able to ensure that garlic stems of different thicknesses can enter between the two fingers, the distance between the two fingers is larger than the cross-sectional diameter of the garlic stem, which results in a gap between the stem and the fingers. Along the conveying direction, when the garlic stem squeezes finger A, the load cell is under pressure and the output value is negative; when the garlic stem squeezes finger B, the load cell is under tension and the output value is positive. Double round blades were used to cut the roots, and the rotation direction of the double round blades is shown in Figure 9. The conveying speed during cutting was set to 0.75 m/s [16]. The garlic plant after root cutting was performed by the double round blades as shown in Figure 8, and the minimum value of the remaining garlic root length was 1.93 mm.

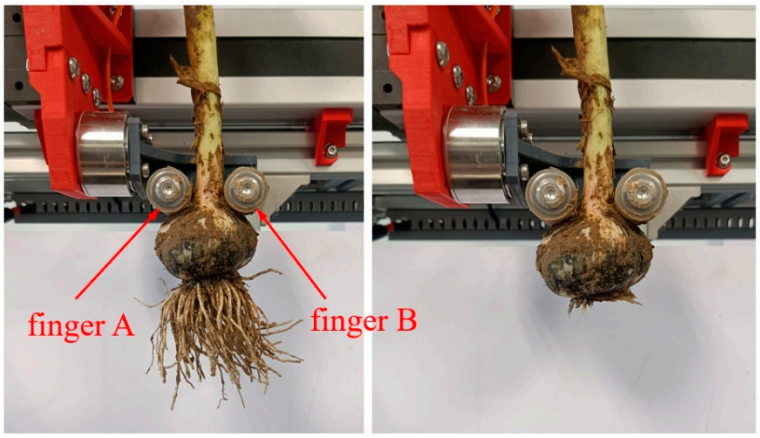

Figure 8. Fingers and the effect of root cutting on the test bench.

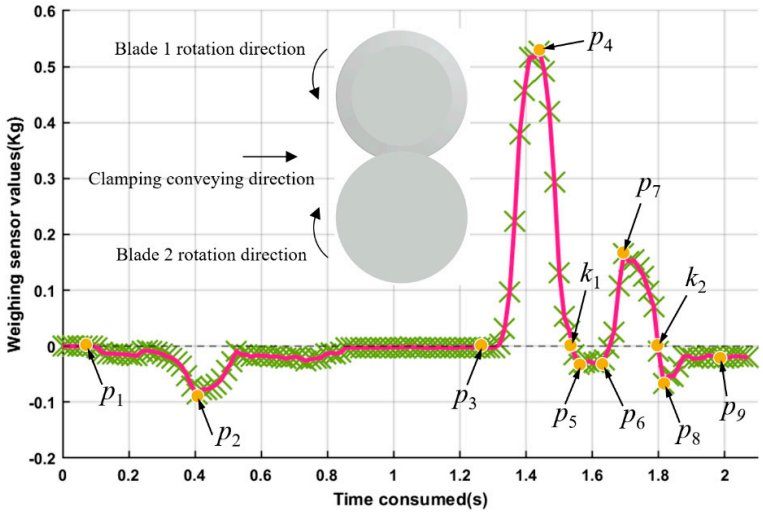

Figure 9. Double round blade root-cutting force curve.

3.1.1. Analysis of the Root-Cutting Process

The force curve of the load cell obtained by rooting with a double round blade is shown in Figure 9. The sampling time interval of the pressure signal is 15 ms, and the sampling duration of the root-cutting process is 2.07 s in total, with 139 sampling points. The cutting line speed of the round blade is 6.908 m/s, which is greater than the clamping and conveying speed. Therefore, the cutting action of the round blade will accelerate the garlic root in the same direction as the external force. It can be seen from Figure 9 that the force curve rises rapidly for the process from point p_3 to point p_4 and from point p_6 to point p_7, indicating that the process of cutting garlic root with the double round blades contains two cutting actions. From the values of the force curve, it can be seen that the first cutting action of the double round blade is stronger than the second cutting action. At the same time, it is known that the process from point p_3 to point p_7 is the process in which the double round blades interact with the garlic roots. In addition, the force curve quantitatively describes the whole root-cutting process, which provides a basis for in-depth analysis.

A key detail of the force profile of the finger will be discussed next to illustrate the important information. The force curve from point p_1 to point p_3 is the acceleration of the garlic plant from rest to the specified conveying speed by the clamping conveyor. The horizontal line segment before point p_3 shows that the test stand has sufficient acceleration distance to reach the specified conveying speed. The force curve gradually decreases from point p_1 to p_2, indicating that the process corresponds to the acceleration of the garlic plant by force, where the garlic stem squeezes finger A, thus putting the load cell under pressure. After the acceleration, the squeezing pressure of the garlic stem on finger A gradually decreases. The p_8 point is similar to the p_2 point, where the garlic stem squeezes finger A and the squeezing pressure reaches a great value. As can be seen from the force curve graph, the process from point p_8 to p_9 is similar to that from point p_2 to p_3, indicating that the force of garlic stem squeezing finger A is gradually decreasing. Therefore, the process of cutting the roots on the test bench can be explained according to the change in the squeezing force of the garlic stem on the finger. Starting from point p_1, the garlic stem accelerated under the force exerted by finger A. The acceleration of the garlic plant increases from point p_1 to p_2, reaching a maximum value at point p_2, after which the acceleration decreases. The point p_3 is where the plant moves at a constant speed according to the specified conveying speed. From p_3 to p_4 is the point where the cutting force of the double round blade acts on the cut of the garlic root, and the cutting force causes the garlic stem to squeeze finger B. The load cell is subjected to a pulling force and the output value is positive. After point p_4, the squeezing pressure of the garlic stem on finger B decreased continuously. From p_4 to p_5, the squeezing pressure of the garlic stem on finger B decreased continuously until zero, and

then the garlic stem started to squeeze finger A. During p_5 to p_6, the squeezing pressure of the garlic stem on finger A remained unchanged, indicating that the length of overlapping area L was set to meet the need for cutting roots. The reason why the garlic stem squeezed finger A during the cutting process of the double round blade was that the garlic plant needed the squeezing pressure to continue to move in the conveying direction. From p_6 to p_7, the squeezing pressure of the garlic stem on finger A decreased until zero, and then the garlic stem started to squeeze finger B. During p_7 to p_8, the squeezing pressure of the garlic stem on finger B decreased until zero, and then the garlic stem started to squeeze finger B. After p8, the squeezing pressure of the garlic stem on finger A decreases continuously.

However, it can be seen from the graph of the force curve that the output values at points p_5 and p_6 are the same, and the output value at point p_8 is smaller than that at points p_5 and p_6. The occurrence of such a situation indicates that the friction between the cutting surface of the garlic root and the surface of the blade during the cutting process of the double round blade hinders the movement of the garlic plant.

The analysis of the force curve revealed that the bulb and garlic stem were always in contact with the fingering during the cutting of the root, but the force relationship was changing. Due to the gap between the garlic stem and the finger, the movement speed of the bulb increased, then decreased, then increased, and then decreased in both cutting processes. The force curve output from the load cell was used to be able to describe the detailed information of the root-cutting process. Therefore, from the above analysis, it is known that during the cutting of garlic roots by the double round blades, the direction of the combined force on the roots is the same as the conveying direction when the force curve is positive, and the direction of the combined force on the roots is opposite to the conveying direction when the force curve is negative. In addition, after the cutting of the garlic root by the double round blades has occurred, the combined force on the garlic root will include the friction between the cutting surface of the garlic root and the surface of the blades, as follows:

$$F_k' = F_1\cos\alpha + F_2\cos\alpha - N_1\sin\alpha - N_2\sin\alpha - F_n - F_\mu \quad (19)$$

where $F_k{}'$ is the component force of the combined force on the root bundle in the positive direction of the y-axis after cutting has occurred, and F_μ is the frictional force between the cutting surface of the garlic root and the blade surface.

Next, the most important process of cutting the root is discussed. In the process of cutting the garlic root by the double round blades, the combined force on the garlic root at point p_3 is F_k, and the blade of the round blade starts to cut the garlic root; the combined force on the garlic root within point p_3 to point p_5 is $F_k{}'$, and the garlic root is subjected to the joint force of the blade and the surface of the blade. The double round blades complete the first cutting of the garlic root at point p_5; the cutting surface of the garlic root crosses the surface of the round blade within point p_5 to point p_6, and since the garlic root is composed of soft root bundles, the action of the blade of the round blade on a single garlic beard is almost negligible. At point p_6, the blade of the double round blade starts to cut the garlic root again; from point p_6 to point p_9, the double round blade completes the second cutting of the garlic root, after which the garlic root leaves the cutting range of the double round blade completely.

During the cutting of the garlic root by the double round blade, there are two points k_1 and k_2 on the force curve where the force values change from positive to negative. The analysis combined with the interaction between the double round blade and the garlic root shows that points k_1 and k_2 have completely different reasons for the change from positive to negative on the force curve. In points p_3 to k_1, the value of the combined force $F_k{}'$ is positive according to Equation (19), indicating that the garlic stem is squeezing finger B. However, in points k_1 to p_5, the garlic root is still within the range of action of the double round blade, and the value of the combined force $F_k{}'$ becomes negative, indicating that the force exerted by the double round blade on the garlic root to impede the movement of the garlic root in the conveying direction acts on finger A. Then, it is necessary to discuss

how the force that hinders the movement of the garlic root in the conveying direction is generated.

Within points k_1 to p_5, the linear velocity of the edge of the round blade is faster than the velocity of the garlic root along the conveying direction, and the action of the edge of the round blade should be to drive the garlic root. However, the normal thrusts N_1 and N_2 of the double round blades on the root whisker bundle are divided in the opposite direction along the conveying direction, which will hinder the movement of the garlic root along the conveying direction. At the moment when the double round blade starts to cut the root bundle, the roots in contact with the double round blade are subjected to the thrust inside the root bundle and can complete the cutting successfully. However, as the double blades cut the roots, the number of uncut roots decreases, and the thrust inside the bundle decreases. The consequence is that the soft root bundles are continuously pushed away from the blades of the round blades while being cut. The result is that the cutting surface of the double round blade is beveled. When the double round blade cuts the root disc, the root disc is also pushed by the double round blade. The thrust of the double round blade still causes the cutting surface to bevel. Since the root plate is hard and not easily deformed, the thrust of the double round blade acting on the root plate results in a stronger squeezing effect on finger A.

Therefore, the first cutting process of the double round blade is the interaction of the inclined garlic root cutting surface with the round blade surface. As the contact area between the inclined garlic root cutting surface and the round blade surface increases, the resistance of the round blade surface to the movement of the garlic root increases. At point P_5, the garlic root cutting surface is in complete contact with the round blade surface, thus causing the value of the force curve within points p_5 to p_6 to remain essentially constant. The test shows that the closer the cutting surface is to the root disk, the greater the force between the cutting surface and the surface of the round blade. This means that the frictional resistance between the root disc and the surface of the round blade is greater than that between the root whisker and the surface of the round blade. The force curve was in the range from point p_5 to p_6, and the minimum value of -0.032 kg was obtained at point p_5. The comprehensive analysis shows that the double round blades cutting garlic roots have the problem of not cutting cleanly enough to ensure the neat cutting surface of garlic roots. In addition, the reason why the k_2 point on the force curve changed from positive to negative was that the double round blade finished disengaging from the garlic root after completing the second cut. At the same time, the value of point p_9 on the force curve is smaller than that of point p_1, which indicates that the process of cutting the roots has changed the squeezing state of the bulb and the garlic stem on the paddle finger, and the squeezing pressure on finger A after the end of cutting the roots is greater than that before cutting the roots.

3.1.2. Round Blade Root-Cutting Test Results

As can be seen in Figure 10, the force curve of the load cell still shows a double peak with two cuts under the same test conditions. However, the cutting surface of the garlic roots showed a significant inclination due to the thrust of the double round blades. In Figure 10, the minimum lengths of the remaining garlic roots were 9.31 mm and 13.04 mm; as seen in the force curve, the valley between the two peaks during the two cuts did not stabilize in a negative state, which also proved that the soft root bundles could not transmit the thrust of the double round blades to the finger. In actual production, the inclined cutting surface would result in the ineffective removal of the garlic roots and the inability to accurately control the remaining length of the remaining garlic roots cannot be accurately controlled [49]. For precision agriculture, it is important to find a method that can effectively control the length of the remaining garlic roots.

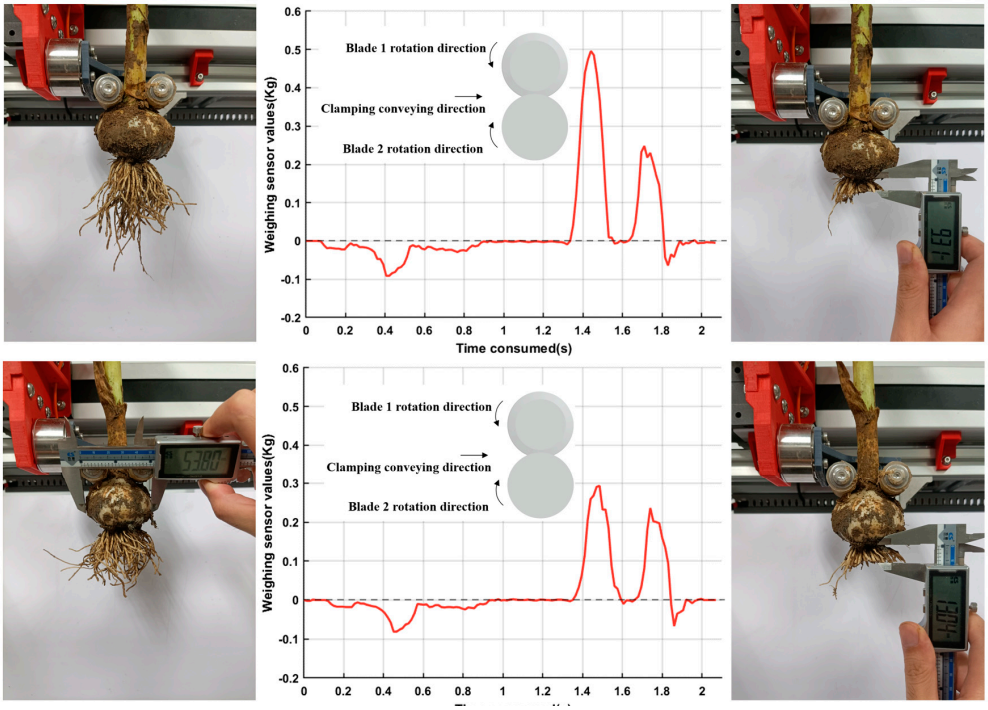

Figure 10. Root-cutting force curve and cutting effect of double round blades.

This study also analyzed the root-cutting test with different rotations of the double round blades. The rotation direction of the double round blades is shown in Figure 11, and the component of the blade linear velocity of the two blades in the overlapping area in the conveying direction is opposite to the direction of the clamping conveying velocity. Garlic specimens of different sizes and shapes were selected for the root-cutting test, as shown in Figure 12. To test the cutting effect of different cutting heights, cutting heights of 2.97 mm, 10.57 mm, 12.44 mm, 6.93 mm, and 12.50 mm were taken for the test. The residual lengths of corresponding cutting heights were 1.47 mm, 8.23 mm, 11.35 mm, 5.03 mm, and 12.27 mm, respectively.

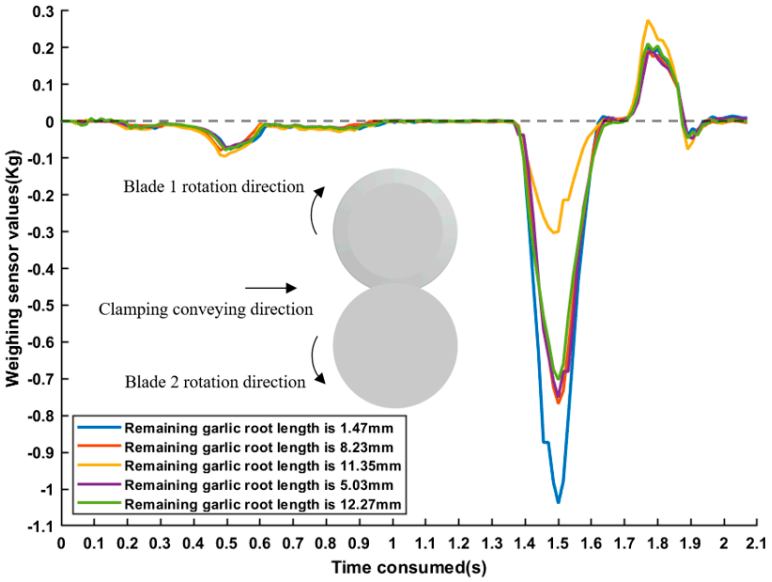

Figure 11. Cutting force curve of double round blades at different cutting heights.

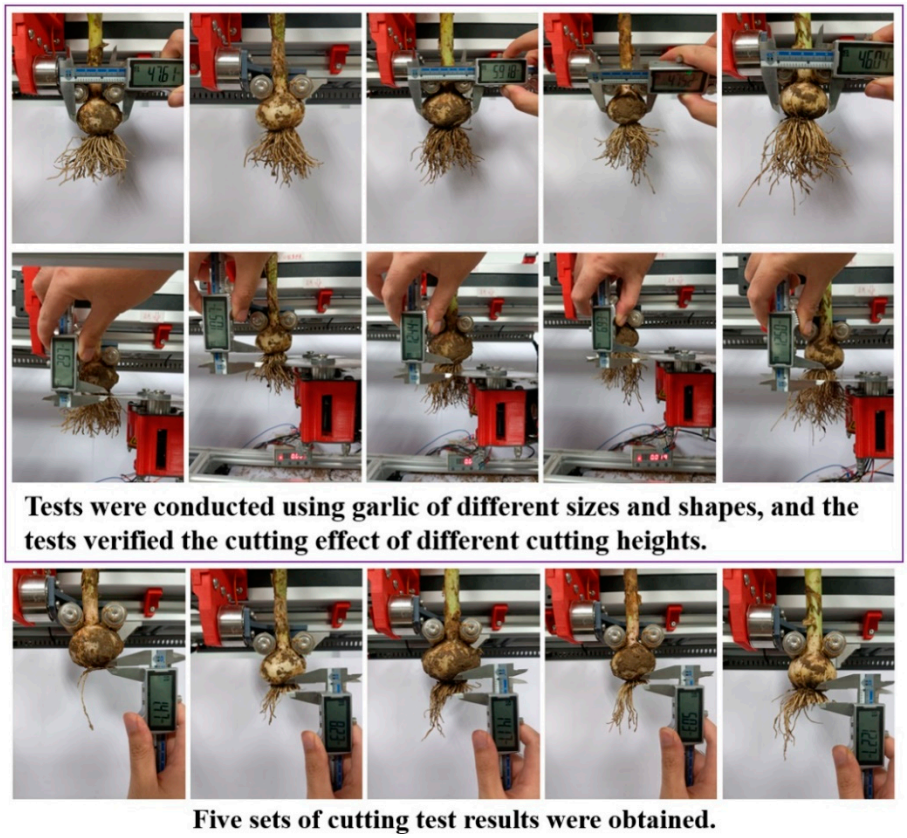

Figure 12. Comparison of cutting effect of double round blades.

The curve in Figure 11 shows the force curve of the load cell obtained by conducting five tests. It can be seen that the force curve has changed significantly. The first trough in the force curve after the occurrence of cutting is negative, and the second peak is positive. The impact of cutting the garlic root was greater due to the increase in relative cutting speed, which resulted in a significant increase in the absolute value of the first trough. When the first cut occurred with the double round blade, the garlic root was subjected to the head-on impact of the double round blade, and the impact of the double round blade caused a rapid surge in the squeezing force on finger A. As the first cut proceeded, the squeezing pressure on finger A reached a peak and then began to gradually decrease. In between the two cuts, there is a state where the extrusion pressure on finger A and finger B is zero. After the start of the second cut, the squeezing force on finger B first increases and then decreases. The force curve stabilized around the zero value after fluctuation. The test results showed that the double round blade was rotated in the direction of Figure 11, and the squeezing force on finger A was greater (the maximum impact was 1.039 kg), which means that the impact generated was greater.

The test results are shown in Figure 12; the cutting effect was not satisfactory, and there was a large number of longer root whiskers that were not removed, which seriously affected the root cutting quality. Additionally, this verifies that the outward thrust of the double round blades on the garlic roots has an unfavorable influence on cutting the roots, and methods should be found to overcome this unfavorable influence.

3.2. Round Blade for Edge Grooving

By analyzing the root-cutting process of double round blades, it is clear that the outward thrust of double round blades on garlic roots has an unfavorable influence factor for cutting roots. Therefore, how to eliminate the outward thrust of the double round blades on the garlic roots is the focus of the research. On the basis of the verification of a large number of practice tests, we proposed slotted round blades. The use of double-slotted

round blades for cutting roots and the use of tooth grooves to bring garlic roots into the overlapping area can effectively eliminate the adverse effect of the outward thrust of double round blades.

The difference between a double-slotted round blade and a double round blade is only that the blade has an inclined V-shaped slot at the edge. After preliminary tests, the number of slanted V-grooves on the slotted round blade was determined to be 35, the depth of the grooves was 7 mm, and the angle of slanting was 35°, as shown in Figure 13. To investigate the root-cutting effect of different blades, slanted blades and straight blades were studied. The root beard bundle and the blade moved in the direction of the arrow in Figure 13. When the slotted round blade was used for root cutting, the slotted round blade was able to produce a downward thrust F_{ki} on the garlic root in the gathering area of the garlic root. The direction of the downward thrust F_{ki} was perpendicular to the blade of the slotted part, and the projection in the projection in direction of clamping and conveying is in the same direction as the clamping and conveying direction. The forward thrust on the root bundle is F_k'.

$$F_k' = \sum_i^n F_{ki} \tag{20}$$

where F_{ki} is the ith downward thrust, and the total number of downward thrusts is assumed to be n.

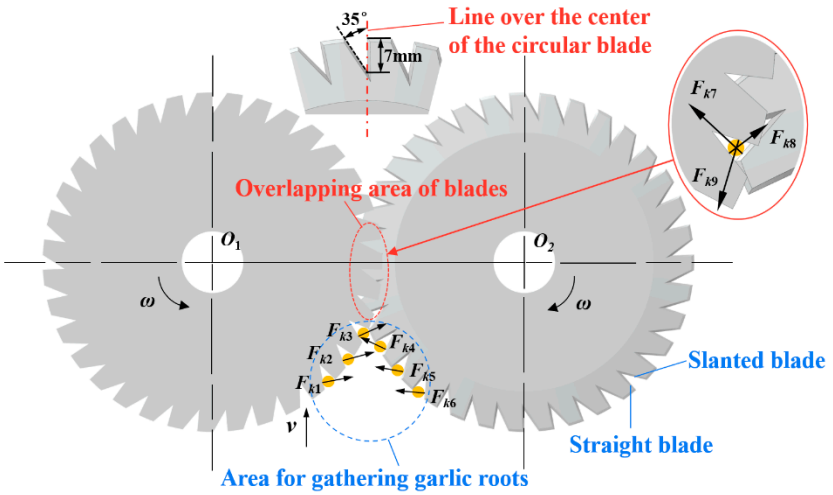

Figure 13. Edge grooving of the round blade root-cutting force.

As the root bundle comes into contact with the double-slotted round blades, the bundle is gathered and brought into the overlapping area of the double blades by a downward thrust. As shown in Figure 13, the double-slotted round blades work together to apply shearing force to the garlic root, producing a shearing effect similar to that of scissors. At the same time, the shearing force exerted by the double-slotted round blades on the garlic root can produce a cutting effect in different directions, thus ensuring that the garlic root is not pushed away by the blades.

It was found through pre-testing that with the slotted round blade with an inclined V-groove, the blade cut the garlic root with a sliding cut instead of a straight cut. The sliding cut ensures that the garlic root is cut while requiring less cutting force. Since different garlic has different root bundles, the force on the garlic roots during root cutting with the double-slotted round blade is too complicated, so the force profile needs to be measured by load cells in the study. The data obtained by the load cell were analyzed quantitatively.

The test bench operation and parameter settings for the double-slotted round blade root cut test are the same as for the double round blade root cut test. The test still needs to be evaluated on the basis of the force curve and the root cut quality of the sample.

The slanted blade and straight blade were used for the root cutting test, and all the test parameters were identical for the slanted blade and straight blade. The results of the

slanted blade and straight blade tests are shown in Figure 14. Simultaneously, the rotation direction of the slotted blade is shown in Figure 14.

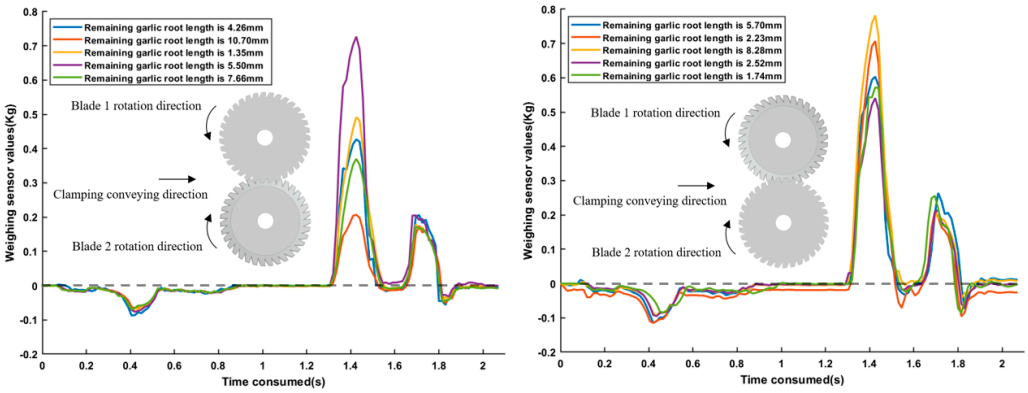

Figure 14. Comparison of force curves for cutting roots with different edges of round blades with grooved edges.

Similarly, the root cutting test of the slanted blade and straight blade tested the cutting effect of different cutting heights. The residual lengths of the slanted blade were 4.26 mm, 10.70 mm, 1.35 mm, 5.50 mm, and 7.66 mm, respectively. The residual lengths of the straight blade were 5.70 mm, 2.23 mm, 8.28 mm, 2.52 mm, and 1.74 mm, respectively. The force curves of the slanted blade and straight blade were obtained by the test.

As can be seen from Figure 14, the force curves of the slanted blade and straight blade are similar to the force curves of double round blades, and both have two cutting processes. The force curves show a saddle shape, consisting of a higher crest and a lower crest as well as a trough between the two crests. The maximum value of the first cut on the finger B squeezing force is significantly larger than the maximum value of the second cut on the finger B squeezing force. It can also be seen from Figure 14 that the maximum values of the first cut on the finger B squeeze for the slanted blade are more dispersed, while the maximum values of the first cut on the finger B squeeze for the straight blade are concentrated at the larger values. The mean value of the maximum value of the first cut of the straight blade on the finger B pressure was 0.4446 kg, and the mean value of the first cut of the straight blade on the finger B pressure was 0.6414 kg. The troughs of the slanted blade have significant fluctuations, and the values of the troughs are small negative values.

According to the previous analysis, the saddle-shaped trough of the force curve can indicate whether the cutting surface of the root is neat or not, which is an important characteristic to measure the quality of the root cut. Therefore, the force curves of the slanted blade and straight blade show that the slanted blade has less cutting force than the straight blade, and the cutting surface is straighter and neater. The slanted blade is less forceful than the straight blade, and the slanted blade produces a neater cut. This result is in line with common sense and shows that the analysis of the force curve is realistic. From the point of view of the cutting effect, a slanted blade is better than a straight blade.

Figure 15 shows the root-cutting test with a double-slotted round blade or slanted blade. Different sizes and shapes of garlic were used for the root-cutting test. To test the cutting effect of different cutting heights, the cutting heights were 4.16 mm, 7.89 mm, 3.31 mm, 4.76 mm, and 5.24 mm, respectively, and the remaining root lengths corresponding to the cutting heights were 4.26 mm, 10.70 mm, 1.35 mm, 5.50 mm, and 7.66 mm, respectively. The root whiskers and the cut were straight. At the same time, the remaining root whiskers were plucked and presented in the same direction as the clamping and conveying direction, which also verified that the thrust of the round blade on the garlic root with the double slotting facilitated the removal of the garlic root. The test results indicate that the double-slotted round blade cuts better than the double-rounded blade.

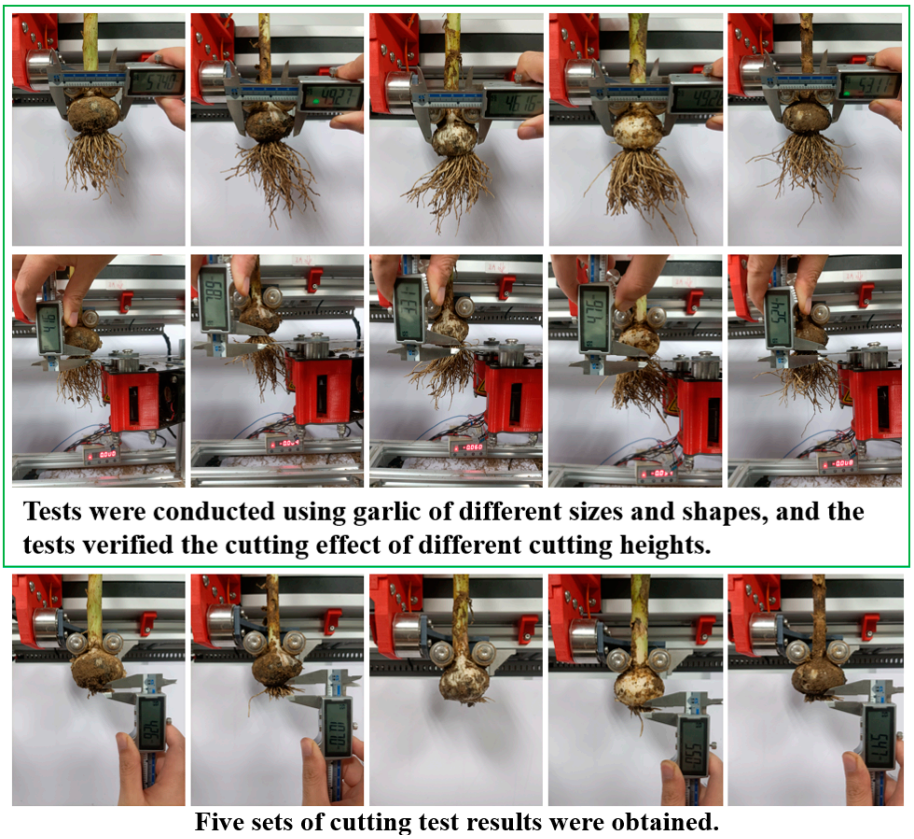

Figure 15. Comparison of cutting effect of a double round blade with edge grooving.

4. Discussion

Automated root cutting of garlic is the key technology that restricts the full mechanization of the garlic industry. Chen et al. [50] designed a linkage occlusion cutting mechanism, performed a garlic disk cutting force test, quantified and analyzed the cutting process using pressure sensors, and plotted the cutting force curve to obtain the optimal tool parameters. Barman et al. [51] developed garlic stem cutting equipment for replacing manual labor, which can perform feeding, clamping, cutting, and collecting operations, effectively improving work efficiency, but did not analyze the cutting process. Tang et al. [52] carried out bionic optimization of the carrot stem and leaf cutting cutter disc on a carrot combine harvester, established kinematic and kinetic models of the cutter, stem, and leaf, and verified the optimization effect by field harvesting tests. Levshin et al. [53] studied the cutting mechanism of potato shoots using a disc knife and showed that cutting separation was better under supported conditions. Momin et al. [54] studied the quality of sugarcane stem cutting by comparing various disc knives to obtain the optimal blade configuration parameters. Currently, the cutting of tough objects, such as stalks, has been studied more thoroughly, but less research has been conducted on the cutting of flexible objects, such as the roots of garlic. This paper not only analyzes the force of the root-cutting process but also quantifies the force variation of the cutting process with the help of pressure sensors. An effective method for analyzing the cutting process of agricultural products is provided, and the whole cutting process of garlic roots by double round blades is clarified.

The present study provides experimental innovations, but there are some limitations. Due to the limitations of objective factors such as time and conditions, experimental studies on different varieties of garlic are lacking. Secondly, this study was conducted only on samples treated with preservation; however, the physical properties of garlic roots with different moisture contents varied greatly. Therefore, the adaptability of the method needs to be verified for samples of different varieties and water contents in subsequent studies. In addition, this paper is an experimental study based on a test bench and does not consider

the effect of actual field operating conditions on the cutting effect. In the next study, the cutting effect under combined harvesting operation conditions of garlic will be further investigated.

5. Conclusions

The structural parameters of garlic cutting blades were designed and optimized in this study to improve the cutting effect of cutting round blades when cutting roots of garlic. To address the problem that the force relationship between the garlic root bundle and the cutting blade is difficult to study scientifically, this paper proposes a research method based on continuous force feedback and conducts practical experimental research on different blade forms, different rotation methods, and different edge angles. The pressure sensor is used to sense the change of force on the garlic root and plot the curve to quantify and analyze the force problem which is difficult to study scientifically. Moreover, the theory of using force curves to evaluate the cutting effect proposed in the study was verified by practical experiments.

The analysis of the force curve showed that the saddle-like trough of the force curve is the key area to measure the cutting effect, and the double-slotted round blade with a slanted blade cut better than the double-slotted round blade with a straight blade and the double round blade. The diameter of the round blade was 110 mm, and the speed was 1200 r/min. The mean value of the maximum value of the force curve of the double-slotted round blade of the slanted blade was 0.4446 kg. The double-slotted round blade of the slanted blade had a thrust force that facilitated cutting during the root-cutting process. Using the force sensor with continuous feedback, this research process can provide a reference for force analysis of cutting different agricultural products.

Author Contributions: K.Y., conceptualization, methodology, software, visualization, and writing—original draft; Z.Y., methodology, resources, supervision, funding acquisition, and writing—review and editing; W.L., methodology and software; J.F., software and investigation; Y.L., investigation and methodology; F.G., investigation, methodology, and resources; Y.Z., data curation and project administration; S.W., software, investigation, funding acquisition, and supervision; B.P., methodology and supervision; Z.H., conceptualization, funding acquisition, resources, and writing—review and editing. All authors have read and agreed to the published version of the manuscript.

Funding: This work was supported by the Projects funded by the Jiangsu Modern Agricultural Machinery Equipment and Technology Demonstration and Extension (NJ2020-24), the Jiangsu Modern Agricultural Machinery Equipment and Technology Demonstration and Extension (NJ2021-22), the National Natural Science Foundation of China (52105263), and the National Key R&D Program of China (2017YFD0701305-02).

Data Availability Statement: The data collected in this research are available when required upon reasonable request.

Conflicts of Interest: The authors declare no conflict of interest.

References

1. Tao, Y.; Zhang, J.; Jiang, S.; Xu, Y.; Show, P.; Han, Y.; Ye, X.; Ye, M. Contacting ultrasound enhanced hot-air convective drying of garlic slices: Mass transfer modeling and quality evaluation. *J. Food Eng.* **2018**, *235*, 79–88. [CrossRef]
2. Furdak, P.; Pieńkowska, N.; Bartosz, G.; Sadowska-Bartosz, I. Extracts of Common Vegetables Inhibit the Growth of Ovary Cancer Cells. *Foods* **2022**, *11*, 2518. [CrossRef] [PubMed]
3. Recinella, L.; Gorica, E.; Chiavaroli, A.; Fraschetti, C.; Filippi, A.; Cesa, S.; Cairone, F.; Martelli, A.; Calderone, V.; Veschi, S.; et al. Anti-Inflammatory and Antioxidant Effects Induced by *Allium sativum* L. Extracts on an Ex Vivo Experimental Model of Ulcerative Colitis. *Foods* **2022**, *11*, 3559. [CrossRef] [PubMed]
4. Thomas, A.; Boobyer, C.; Borgonha, Z.; van den Heuvel, E.; Appleton, K.M. Adding Flavours: Use of and Attitudes towards Sauces and Seasonings in a Sample of Community-Dwelling UK Older Adults. *Foods* **2021**, *10*, 2828. [CrossRef]
5. Han, C.; Liu, J.; Chen, K.; Lin, Y.; Chen, C.; Fan, C.; Lee, H.; Liu, D.; Hou, W. Antihypertensive activities of processed garlic on spontaneously hypertensive rats and hypertensive humans. *Bot. Stud.* **2011**, *52*, 277–283.

6. Wang, J.; Zhang, X.; Lan, H.; Wang, W. Effect of garlic supplement in the management of type 2 diabetes mellitus (T2DM): A meta-analysis of randomized controlled trials. *Food Nutr. Res.* **2017**, *61*, 1377571. [CrossRef]
7. Phan, A.D.T.; Netzel, G.; Chhim, P.; Netzel, M.E.; Sultanbawa, Y. Phytochemical Characteristics and Antimicrobial Activity of Australian Grown Garlic (*Allium sativum* L.) Cultivars. *Foods* **2019**, *8*, 358. [CrossRef]
8. Shrestha, D.K.; Sapkota, H.; Baidya, P.; Basnet, S. Antioxidant and Antibacterial Activities of Allium sativum and Allium cepa. *Bull. Pharm. Res.* **2016**, *6*, 50–55.
9. Ghani, M.I.; Ali, A.; Atif, M.J.; Ali, M.; Amin, B.; Anees, M.; Cheng, Z. Soil Amendment with Raw Garlic Stalk: A Novel Strategy to Stimulate Growth and the Antioxidative Defense System in Monocropped Eggplant in the North of China. *Agronomy* **2019**, *9*, 89. [CrossRef]
10. Nascimento, V.F.; Auad, A.M.; de Resende, T.T.; Visconde, A.J.M.; Dias, M.L. Insecticidal Activity of Aqueous Extracts of Plant Origin on Mahanarva spectabilis (Distant, 1909) (Hemiptera: Cercopidae). *Agronomy* **2022**, *12*, 947. [CrossRef]
11. Netzel, M.E. Garlic: Much More Than a Common Spice. *Foods* **2020**, *9*, 1544. [CrossRef]
12. Pocketbook, F.S. *World Food and Agriculture*; Food and Agriculture Organization: Rome, Italy, 2016.
13. Yu, Z.; Yang, K.; Hu, Z.; Peng, B.; Gu, F.; Yang, L.; Yang, M. Parameter optimization and simulation analysis of floating root cutting mechanism for garlic harvester. *Comput. Electron. Agric.* **2023**, *204*, 107521. [CrossRef]
14. Yang, K.; Yu, Z.; Gu, F.; Zhang, Y.; Wang, S.; Peng, B.; Hu, Z. Experimental Study of Garlic Root Cutting Based on Deep Learning Application in Food Primary Processing. *Foods* **2022**, *11*, 3268. [CrossRef]
15. Yang, K.; Peng, B.; Gu, F.; Zhang, Y.; Wang, S.; Yu, Z.; Hu, Z. Convolutional Neural Network for Object Detection in Garlic Root Cutting Equipment. *Foods* **2022**, *11*, 2197. [CrossRef]
16. Yang, K.; Hu, Z.; Yu, Z.; Peng, B.; Zhang, Y.; Gu, F. Design and Experiment of Garlic Harvesting and Root Cutting Device Based on Deep Learning Object Determination. *Trans. Chin. Soc. Agric. Mach.* **2022**, *53*, 123–132.
17. Ren, D.; Yu, H.; Zhang, R.; Li, J.; Zhao, Y.; Liu, F.; Zhang, J.; Wang, W. Research and Experiments of Hazelnut Harvesting Machine Based on CFD-DEM Analysis. *Agriculture* **2022**, *12*, 2115. [CrossRef]
18. Luo, W.; Wu, F.; Gu, F.; Xu, H.; Wang, G.; Wang, B.; Yang, H.; Hu, Z. Optimization and Experiment of Fertilizer-Spreading Device for Wheat Wide-Boundary Sowing Planter under Full Rice Straw Retention. *Agronomy* **2022**, *12*, 2251. [CrossRef]
19. Li, Y.; Fan, J.; Hu, Z.; Luo, W.; Yang, H.; Shi, L.; Wu, F. Calibration of Discrete Element Model Parameters of Soil around Tubers during Potato Harvesting Period. *Agriculture* **2022**, *12*, 1475. [CrossRef]
20. Li, Z.; Wu, J.; Du, J.; Duan, D.; Zhang, T.; Chen, Y. Experimenting and Optimizing Design Parameters for a Pneumatic Hill-Drop Rapeseed Metering Device. *Agronomy* **2023**, *13*, 141. [CrossRef]
21. Zou, L.; Yuan, J.; Liu, X.; Li, J.; Zhang, P.; Niu, Z. Burgers viscoelastic model-based variable stiffness design of compliant clamping mechanism for leafy greens harvesting. *Biosyst. Eng.* **2021**, *208*, 1–5. [CrossRef]
22. Hwang, S.; Nam, J. DEM simulation model to optimise shutter hole position of a centrifugal fertiliser distributor for precise application. *Biosyst. Eng.* **2021**, *204*, 326–345. [CrossRef]
23. Tang, Z.; Zhang, B.; Wang, M.; Zhang, H. Damping behaviour of a prestressed composite beam designed for the thresher of a combine harvester. *Biosyst. Eng.* **2021**, *204*, 130–146. [CrossRef]
24. Zargar, O.; Pharr, M.; Muliana, A. Modeling and simulation of creep response of sorghum stems: Towards an un-derstanding of stem geometrical and material variations. *Biosyst. Eng.* **2022**, *217*, 1–17. [CrossRef]
25. Zhao, W.; Chen, M.; Xie, J.; Cao, S.; Wu, A.; Wang, Z. Discrete element modeling and physical experiment research on the biomechanical properties of cotton stalk. *Comput. Electron. Agric.* **2023**, *204*, 107502. [CrossRef]
26. Zhao, Z.; Li, Y.; Liang, Z.; Chen, Y. Optimum design of grain impact sensor utilising polyvinylidene fluoride films and a floating raft damping structure. *Biosyst. Eng.* **2012**, *112*, 227–235. [CrossRef]
27. Mu, L.; Liu, Y.; Cui, Y.; Liu, H.; Chen, L.; Fu, L.; Gejima, Y. Design of End-effector for Kiwifruit Harvesting Robot Experiment. In Proceedings of the ASABE Annual International Meeting, Spokane, WA, USA, 16–19 July 2017; p. 1700666. [CrossRef]
28. Szpunar-Krok, E.; Szostek, M.; Pawlak, R.; Gorzelany, J.; Migut, D. Effect of Fertilisation with Ash from Biomass Combustion on the Mechanical Properties of Potato Tubers (*Solanum tuberosum* L.) Grown in Two Types of Soil. *Agronomy* **2022**, *12*, 379. [CrossRef]
29. Stubbs, C.J.; Sun, W.; Cook, D.D. Measuring the transverse Young's modulus of maize rind and pith tissues. *J. Biomech.* **2019**, *84*, 113–120. [CrossRef]
30. Catania, P.; Comparetti, A.; De Pasquale, C.; Morello, G.; Vallone, M. Effects of the Extraction Technology on Pome-granate Juice Quality. *Agronomy* **2020**, *10*, 1483. [CrossRef]
31. Lee, S.; Zargar, O.; Reiser, C.; Li, Q.; Muliana, A.; Finlayson, S.A.; Gomez, F.E.; Pharr, M. Time-dependent mechanical behavior of sweet sorghum stems. *J. Mech. Behav. Biomed. Mater.* **2020**, *106*, 103731. [CrossRef]
32. Lu, W.; Li, X.; Zhang, G.; Tang, J.; Ni, S.; Zhang, H.; Zhang, Q.; Zhai, Y.; Mu, G. Research on Biomechanical Properties of Laver (*Porphyra yezoensis* Ueda) for Mechanical Harvesting and Postharvest Transporta-tion. *AgriEngineering* **2022**, *4*, 48–66. [CrossRef]
33. Chattopadhyay, P.S.; Pandey, K.P. Mechanical Properties of Sorghum Stalk in relation to Quasi-static Deformation. *J. Agric. Eng. Res.* **1999**, *73*, 199–206. [CrossRef]
34. Goonewardena, J.; Ashraf, M.; Reiner, J.; Kafle, B.; Subhani, M. Constitutive Material Model for the Compressive Behaviour of Engineered Bamboo. *Buildings* **2022**, *12*, 1490. [CrossRef]
35. Moya, M.; Sánchez, D.; Villar-García, J.R. Values for the Mechanical Properties of Wheat, Maize and Wood Pellets for Use in Silo Load Calculations Involving Numerical Methods. *Agronomy* **2022**, *12*, 1261. [CrossRef]

36. Szpunar-Krok, E.; Kuźniar, P.; Pawlak, R.; Migut, D. The Effect of Foliar Fertilization on the Resistance of Pea (*Pisum sativum* L.) Seeds to Mechanical Damage. *Agronomy* **2021**, *11*, 189. [CrossRef]
37. Gagliardi, L.; Fontanelli, M.; Frasconi, C.; Sportelli, M.; Antichi, D.; Tramacere, L.G.; Rallo, G.; Peruzzi, A.; Raffaelli, M. Assessment of a Chain Mower Performance for Weed Control under Tree Rows in an Alley Cropping Farming System. *Agronomy* **2022**, *12*, 2785. [CrossRef]
38. Zhang, Z.; Zhou, J.; Yi, B.; Zhang, B.; Wang, K. A flexible swallowing gripper for harvesting apples and its grasping force sensing model. *Comput. Electron. Agric.* **2023**, *204*, 107489. [CrossRef]
39. Ding, A.; Peng, B.; Yang, K.; Zhang, Y.; Yang, X.; Zou, X.; Zhu, Z. Design of a Machine Vision-Based Automatic Digging Depth Control System for Garlic Combine Harvester. *Agriculture* **2022**, *12*, 2119. [CrossRef]
40. Erukainure, F.E.; Parque, V.; Hassan, M.A.; FathEl-Bab, A.M.R. Estimating the stiffness of kiwifruit based on the fusion of instantaneous tactile sensor data and machine learning schemes. *Comput. Electron. Agric.* **2022**, *201*, 107289. [CrossRef]
41. Huang, M.; He, L.; Choi, D.; Pecchia, J.; Li, Y. Picking dynamic analysis for robotic harvesting of Agaricus bisporus mushrooms. *Comput. Electron. Agric.* **2021**, *185*, 106145. [CrossRef]
42. Wang, C.; Zang, X.; Zhang, X.; Liu, Y.; Zhao, J. Parameter estimation and object gripping based on fingertip force/torque sensors. *Measurement* **2021**, *179*, 109479. [CrossRef]
43. Wang, C.; Zang, X.; Zhang, H.; Chen, H.; Chen, H.; Lin, Z.; Zhao, J. Status Identification and Object In-Hand Reorientation Using Force/Torque Sensors. *IEEE Sens. J.* **2021**, *21*, 20694–20703. [CrossRef]
44. Payo, I.; Adánez, J.M.; Rosa, D.R.; Fernández, R.; Vázquez, A.S. Six-Axis Column-Type Force and Moment Sensor for Robotic Applications. *IEEE Sens. J.* **2018**, *18*, 6996–7004. [CrossRef]
45. Wang, Y.; Yang, Y.; Zhao, H.; Liu, B.; Ma, J.; He, Y.; Zhang, Y.; Xu, H. Effects of cutting parameters on cutting of citrus fruit stems. *Biosyst. Eng.* **2020**, *193*, 1–11. [CrossRef]
46. Jin, X.; Du, X.; Wang, S.; Ji, J.; Dong, X.; Wang, D. Design and Experiment of Stems Cutting Device for Carrot Harvester. *Trans. Chin. Soc. Agric. Mach.* **2016**, *47*, 82–89. [CrossRef]
47. Yu, Z.; Hu, Z.; Yang, K.; Peng, B.; Wu, F.; Xie, H. Design and experiment of root cutting device in garlic combine harvesting. *Trans. CSAE* **2016**, *32*, 77–85. [CrossRef]
48. Yu, Z.; Hu, Z.; Yang, K.; Peng, B.; Zhang, Y.; Yang, M. Operation Mechanism Analysis and Parameter Optimization of Garlic Root Floating Cutting Device. *Trans. Chin. Soc. Agric. Mach.* **2021**, *52*, 111–119. [CrossRef]
49. Du, Z.; Li, D.; Ji, J.; Zhang, L.; Li, X.; Wang, H. Bionic Optimization Design and Experiment of Reciprocating Cutting System on Single-Row Tea Harvester. *Agronomy* **2022**, *12*, 1309. [CrossRef]
50. Chen, J.; Zhou, B.; Jia, J.; Chen, Z.; Yu, C.; Cai, S. Design and parameters optimization of root cutting tool based on garlic numerical simulation model. *Food Process Eng.* **2021**, *44*, e13753. [CrossRef]
51. Barman, C.; Bhatt, Y.C.; Jain, H.K.; Vyas, S.S. Performance Evaluation of Power Operated Garlic Stem and Root cutter. *Agric. Eng. Today* **2015**, *39*, 57–61.
52. Tang, H.; Jiang, Y.; Wang, J.; Guan, R.; Zhou, W. Bionic Design and Parameter Optimization of Rotating and Fixed Stem- and Leaf-Cutting Devices for Carrot Combine Harvesters. *Math. Probl. Eng.* **2021**, *2021*, 1–4. [CrossRef]
53. Levshin, A.; Gasparyan, I.; Shchigolev, S.; Mekhedov, M. Design of cutting device for decapitation of potato shoots. *Eng. Rural. Dev.* **2021**, *5*, 26–28. [CrossRef]
54. Momin, M.A.; Wempe, P.A.; Grift, T.E.; Hansen, A.C. Effects of Four Base Cutter Blade Designs on Sugarcane Stem Cut Quality. *Trans. ASABE* **2017**, *60*, 1551–1560. [CrossRef]